



Research article

One-pot hydrothermal synthesis of a magnetic hydroxyapatite nanocomposite for MR imaging and pH-Sensitive drug delivery applications

Mehraneh Kermanian^{a,b}, Mehran Naghibi^c, Somayeh Sadighian^{a,b,*}^a Zanjan Pharmaceutical Nanotechnology Research Center, School of Pharmacy, Zanjan University of Medical Sciences, Zanjan, Iran^b Department of Pharmaceutical Biomaterials, School of Pharmacy, Zanjan University of Medical Sciences, Zanjan, Iran^c Department of Anatomical Sciences, Faculty of Medicine, Tabriz University of Medical Sciences, Tabriz, Iran

ARTICLE INFO

Keywords:

MRI
T2-contrast agent
Hydroxyapatite
Magnetite
Hydrothermal synthesis
pH-sensitivity
Nanocomposites
Nanomaterials
Nanoparticle synthesis
Nanostructure
Nanotechnology
Pharmaceutical chemistry
Inorganic chemistry

ABSTRACT

Synthetic hydroxyapatite (HA) due to its high biocompatibility, anti-inflammatory properties, high stability, and a flexible structure in combination with magnetic nanoparticles has the strong potential to be used in modern medicine including tissue engineering, imaging, and drug delivery. Herein, a hydrothermal process was used to prepare magnetite nanoparticles dispersed on the hydroxyapatite nanorods with cetyltrimethylammonium bromide (CTAB) as a surfactant. Characterization study of the synthesized iron oxide-hydroxyapatite (IO-HA) nanocomposite was performed by FT-IR spectroscopy, X-ray powder diffraction, energy dispersive X-Ray analysis (EDX) for elemental mapping, transmission electron microscopy, and vibrating sample magnetometer. Then, the biocompatibility of the synthesized nanocomposite studied by 3-(4,5-dimethylthiazol-2-yl)-2,5-diphenyltetrazolium bromide (MTT) assay and hemocompatibility assay. Focus on this point, curcumin loaded IO-HA (Cur@IO-HA) was developed for exploring the pH-sensitivity of the drug carrier and then evaluating its cellular uptake. The *in vitro* efficacy of the synthesized nanocomposites as a magnetic resonance imaging (MRI) contrast agent was also investigated. Our results showed that IO-HA nanocomposite is non-cytotoxic and hemocompatible as well as a good pH-sensitive drug carrier and a favorable MRI T2 contrast agent. Comparing to the free curcumin, Cur@IO-HA displayed a good cellular uptake. Taking into account the above issues, IO-HA nanocomposite has the most potential for application as a theranostic MRI contrast agent.

1. Introduction

Magnetic nanoparticles (MNP) have been extensively regarded and studied due to their various applications in medical fields such as gene/drug delivery system [1], cancer hyperthermia therapy [2], imaging tumors [3], normal and damaged tissues with MRI technique [4] and intracellular imaging [5] (see Scheme 1).

Magnetic resonance imaging (MRI) is a non-invasive clinical imaging technique. Studies have shown that the use of magnetic nanoparticles in MRI provides better contrast of images and allows for imaging at the cellular and molecular levels. MRI contrast in tissues is caused by differences in proton density, spin-lattice relaxation time (T1), and spin-spin relaxation time (T2). In most tissues, the intrinsic changes of T1 and T2 are small and are often used in clinical applications to enhance the contrast between the target and surrounding tissues. Depending on whether the contrast agent-induced shortening of relaxation time is greater for T1 (longitudinal) or T2 (transverse) relaxation, MRI contrast

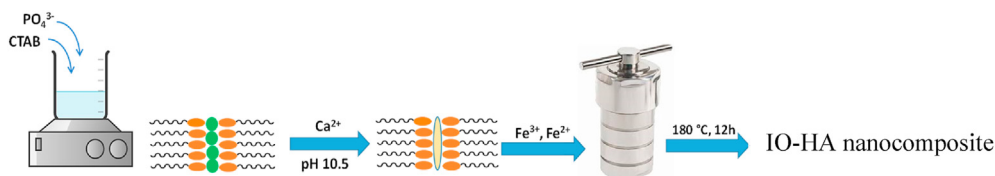
agents are described as either “T1 agents” or “T2 agents” [6]. T1 contrast agents were based on gadolinium and manganese, which increased the signal in the nanoparticle aggregation regions, and these areas were seen brighter than adjacent tissues in the image [7]. Whereas T2 contrast agents are based on iron oxide nanoparticles and attenuate signal intensity results in darker T2 weight images [8].

Although gadolinium chelates are widely used in their short circulation time, poor tracking sensitivity and their toxicity have led to the continuous development of iron oxide nanoparticles as contrast agents [9].

In recent years, the magnetite nanoparticles (Fe₃O₄) with a cubic inverse spinel structure have been considered as a contrast agent for the diagnosis and treatment of cancer disease. Until now, finding suitable synthetic strategies with high reproducibility to have Fe₃O₄ nanoparticles with desirable size and tunable magnetic properties is a great challenge [2]. On the other hand, to diminish the biofouling and intrinsic aggregation of iron oxide nanoparticles due to the ubiquitous Van der

* Corresponding author.

E-mail addresses: somayeh.sadighian@gmail.com, sadighian@zums.ac.ir (S. Sadighian).



Scheme 1. Synthetic Procedure of IO-HA nanocomposite.

Waals forces, it is necessary to modify the nanoparticle surface in biological conditions [10]. There are various methods to modify the surface of Fe_3O_4 nanoparticles, including the use of ceramics, polymers, composites, etc.

So far, extensive studies have been undertaken to fabricate nano-scaled MRI contrast agents to be effective and efficient in clinical therapies, especially hybrid magnetic nanocomposites [11,12].

Although many inorganic materials have been studied for this purpose, hydroxyapatite ($\text{Ca}_{10}(\text{PO}_4)_6(\text{OH})_2$ or HA) is the most suitable inorganic coating material [13]. Hydroxyapatite is a natural mineral form of calcium apatite. The well-known characteristics of HA include biocompatibility, unique mechanical properties, bioactivity, non-inflammatory properties, and excellent ability to form chemical bonds with living bone tissue [14]. Since hydroxyapatite is a major component of hard tissues such as teeth and bones, concerning its specific features mentioned above, the applications of its different functionalized derivatives with various morphologies for use in various fields such as medical diagnosis [15] and tissue engineering [16] are highly regarded [17]. Hydroxyapatite, however, can be a favorable material as a drug carrier for drug delivery purposes [18], since its excellent biocompatibility and pH-sensitive characteristics which can be degraded into calcium and phosphorous elements under weakly acidic conditions [18,19].

Considering the above issues, the main objective of this study was to prepare and characterize the nanocomposite of hydroxyapatite and iron oxide by hydrothermal method and evaluate its potential as an MRI contrast agent concerning its cytotoxic and hemolytic properties. Also, the potential of this nanocomposite as a pH-sensitive drug carrier was studied *in vitro* for curcumin delivery as a model drug. Curcumin as a major component of the turmeric (*Curcuma longa*) plant that has anti-cancer properties and some limitations such as low bioavailability, poor solubility, rapid metabolism, rapid systemic elimination in the free form [20]. In this study, the synthesized nanocomposite, IO-HA, was used for curcumin delivery to overcome these limitations.

2. Experimental

2.1. Materials

Ferric chloride hexahydrate ($\text{FeCl}_3 \cdot 6\text{H}_2\text{O}$), ferrous chloride tetrahydrate ($\text{FeCl}_2 \cdot 4\text{H}_2\text{O}$), Calcium chloride dihydrate ($\text{CaCl}_2 \cdot 2\text{H}_2\text{O}$), diammonium hydrogen phosphate ($(\text{NH}_4)_2(\text{HPO}_4)$), Cetyl trimethylammonium bromide (CTAB), ammonium hydroxide (NH_4OH) and the other reagents all were purchased locally from Sigma-Aldrich Chemicals and used as received.

2.2. Synthesis of magnetic hydroxyapatite (IO-HA)

The hydrothermal process was used for the synthesis of the magnetic nanocomposite according to the previous report [20,21]. Typically, 0.01 M of $(\text{NH}_4)_2\text{HPO}_4$ and 0.1 M of CTAB was dissolved in distilled water at room temperature with continuous stirring. Then, a solution of $\text{CaCl}_2 \cdot 2\text{H}_2\text{O}$ (0.03 M) in distilled water was prepared. Further, the CTAB-phosphate solution was added dropwise to the calcium chloride solution and adjusts the pH to 10.5 by adding the ammonium hydroxide (30%) with vigorous stirring for 60 min. Simultaneously, an aqueous solution $\text{FeCl}_2 \cdot 4\text{H}_2\text{O}$ and $\text{FeCl}_3 \cdot 6\text{H}_2\text{O}$ with the molar ratio of 1:1.5 for

Fe^{2+} and Fe^{3+} was prepared and the pH was adjusted 12 by ammonium hydroxide (30%). Then the two prepared solutions were mixed and stirred for 20 min. The final mixture further transferred to the Teflon-lined stainless-steel autoclave and kept in an oven at 180°C for 12 h. After cooling down to room temperature, the supernatant was removed by centrifugation at 19000 rpm for 20 min followed by washing the precipitate by ethanol and water several times. The final brown color precipitate was dried at 70°C under vacuum to obtain the IO-HA nanocomposite.

2.3. Preparation of curcumin loaded IO-HA (Cur@IO-HA)

Curcumin was loaded on the IO-HA nanocomposite via a previously reported method [22]. In detail, 20 mg of the nanoparticles were dispersed in 10 ml of distilled water under stirring at 400 rpm. 4.0 mg of curcumin was dissolved in 100 μL of acetone and added dropwise to the suspension. The mixture was kept stirring (200 rpm) for 24 h at room temperature. The resulting curcumin-loaded nanoparticles were collected with an external magnet and washed with distilled water. To determine the loading efficiency, 5.0 mg of curcumin-loaded particles were suspended in 10 mL of ethanol. The samples were left shaking at room temperature for 24 h and then placed on an external magnet to let the nanoparticles to settle. Afterward, the upper liquid was separated by using a pipette and its absorbance intensity was measured at a wavelength of 427 nm by a UV-visible spectrometer.

2.4. Solid-state characterization

The samples were characterized by different analytical techniques. Fourier transforms infrared (FT-IR) spectra were collected on an FT-IR spectrometer (Bruker, Tensor 27, Biotage, Germany). The spectra were recorded from 4000 to 400 cm^{-1} . The crystalline structures were analyzed by an X-ray powder diffractometer (Bruker, D8 ADVANCE, Germany) using $\text{Cu K}\alpha$ radiation ($\lambda = 1.54178 \text{ \AA}$). The pattern was recorded over 2θ range from 10° to 70° with a step size of $0.0100^\circ/\text{s}$. Vibrating sample magnetometer (VSM) was used to study the magnetic properties of the synthesized nanocomposite at room temperature. The size and morphology of the nanoparticles were investigated by transmission-electron microscope (TEM, FEI Tecnai G20). The elemental composition of the nanocomposite was analyzed by EDS spectroscopy (TESCAN, MIRA III, Czechia). Quantitative results of cellular uptake of the nanoparticles were obtained by a microplate reader (ELISA, Infinite M200). The amount of drug-loaded on and released from the nanoparticles were determined spectrophotometrically at the wavelength of 420 nm (GENESYS™ 10S, Thermo Fisher Scientific, USA).

2.5. Curcumin release study

The release of curcumin from IO-HA nanocomposite was performed in phosphate buffer saline (PBS) with different pH of 5.5 and 7.4 containing 1% v/v tween 80. The whole system was shaken at 100 rpm and 37°C in a shaker-incubator (SI-1000, Heidolph, Germany). Then, at a specified interval (*i.e.* 0.5, 1, 2, 4, 8, 24 h), 1ml of the solution was removed for spectrophotometric measurement and the same amount of buffer/tween was replaced. The amount of releasing curcumin was measured using a UV spectrophotometer at 427 nm [23,24].

2.6. Cellular uptake

MCF-7 cells were used for this study. First, cells were seeded in a 6-well plate at a density of 3×10^5 cells per each well using RPMI with 10% FBS (fetal bovine serum) as a cell culture medium. The cells were incubated with $40 \mu\text{gml}^{-1}$ of free curcumin, 0.8 mg ml^{-1} of Cur@IO-HA nanoparticles, and IO-HA at 37°C and $\%5 \text{ CO}_2$ for 6 h. After incubation, cells were washed with PBS and centrifuged for three minutes. Then the supernatants were removed and washing the plates by PBS three times. Finally, one ml methanol was added to the plates and kept shaking by the vortex. After five minutes, the suspensions were centrifuged for five minutes and the fluorescence intensity of the supernatants was read by ELISA.

2.7. Blood compatibility evaluation

According to the previous report [25], first, the human red blood cells (RBC) were separated from the serum by centrifuge and washed three times with sterile PBS (pH 7.4). Then, 0.5 ml IO-HA nanoparticle suspension in PBS (pH 7.4) with various concentrations of 0.25, 0.5 and 2.5 mg ml^{-1} were added to 0.5 ml of diluted RBC in PBS (pH 7.4). For negative and positive controls, PBS (pH 7.4) and deionized water were used, respectively. All the samples were shaken gently in a shaker incubator at 37°C for 4 h and then centrifuged at 4000 rpm for 5 min. Finally, the absorbance of the supernatant was determined at 540 nm. Hemolysis of red blood cells was calculated by the equation Eq. (1):

$$H(\%) = \frac{A_s - A_n}{A_p - A_n} \times 100 \quad (1)$$

where H is the calculated hemolysis of red blood cells, A_s is the absorbance of the sample and A_p and A_n is the absorbance of the positive and negative control, respectively.

2.8. In vitro cytotoxicity assay

Methyl thiazolyl tetrazolium (MTT) assay was carried out to investigate the Cytotoxicity of IO-HA, Cur@IO-HA, and free curcumin. A breast cancer cell line (MCF-7) was used. Typically, cells were cultured in 96-well plates at a density of 2.0×10^4 cells per each well. The culture media was RPMI with 10% FBS. After 24 h of incubation ($T = 37^\circ\text{C}$, $\text{CO}_2 \%$ 5), cells were treated with various concentrations of free curcumin, Cur@IO-HA, and IO-HA and placed in the incubator for 48 and 72 h. Afterward, the medium was removed and $20 \mu\text{L}$ MTT reagent (5 mgml^{-1}) was added to each well. After 4 h of incubation, $100 \mu\text{L}$ DMSO was added to the wells to dissolve the produced formazan. The absorbance was read by a microplate reader at 570 nm.

2.9. MRI relaxation properties measurements

MR relaxation properties were carried out using a 1.5 T clinical MRI scanner (Siemens Medical Solutions, Erlangen, Germany). For in vitro MRI measurement, suspensions of synthesized nanoparticles with concentrations ranged from 0.05 to 0.25 mM were prepared and placed in a phantom for imaging. A spin-echo sequence was utilized for the measurement of the T2 relaxation time of the samples. The T2 measurement parameters were as follows: repetition time $\text{TR} = 3000 \text{ ms}$, echo time $\text{TE} = 13.8\text{--}220.8 \text{ ms}$, and flip angle $= 180^\circ$.

2.10. Image analysis

The data were processed and analyzed using software MIPAV from the National Institutes of Health (NIH). T2 was calculated by fitting the raw data with the equation Eq. (2):

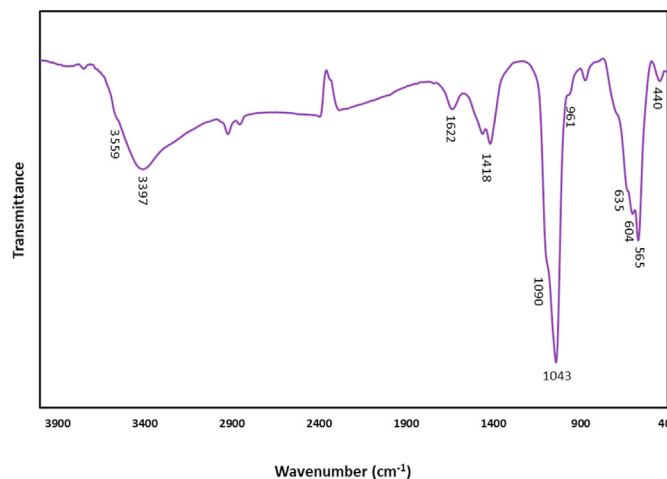


Figure 1. FT-IR spectrum of IO-HA nanocomposite.

$$I = M_0 \exp\left(-\frac{TE}{T_2}\right) \quad (2)$$

where M_0 is the extrapolated signal at $\text{TE} = 0$ and the I is signal measured at each TE .

3. Result and discussion

3.1. Characterization

Figure 1 shows the FT-IR spectrum of the IO-HA nanocomposite. The observed peaks at 440, 565, and 604 relate to the bending vibration of phosphate groups (PO_4^{3-}) while the absorption bands at 961, 1043, and 1090 cm^{-1} correspond to the stretching vibrations of PO_4^{3-} . The bands at 3559 and 635 cm^{-1} are assigned to the vibrations of OH groups at the hydroxyapatite site. The peaks correspond to the H_2O present in the synthesized nanocomposite were appearing around 3397 and 1622 cm^{-1} . These data demonstrate incorporation of Fe_3O_4 did not affect the structure of hydroxyapatite during the synthesis process and is in good accordance with the previous report [20,26].

X-ray diffraction (XRD) spectroscopy is helpful to determine the phases and crystal structure of the IO-HA nanocomposite. As shown in Figure 2. The characteristic peaks appeared in 31.94, 32.11, 32.94, 39.98, 46.68, 49.54 and 53.11 are assigned to (002), (211), (112), (300), (202), (310), (222), (213) and (004) crystal planes of HA (JCPDS card: No. 09-0432). Also, the crystal planes of Fe_3O_4 revealed at 30.23, 35.7, 43.43, 57.40, and 62.95 which correspond to (220), (311), (400), (511), and (440) planes [27], respectively (JCPDS card: No. 89-0688). The results confirm that the crystalline structures of HA and Fe_3O_4 are

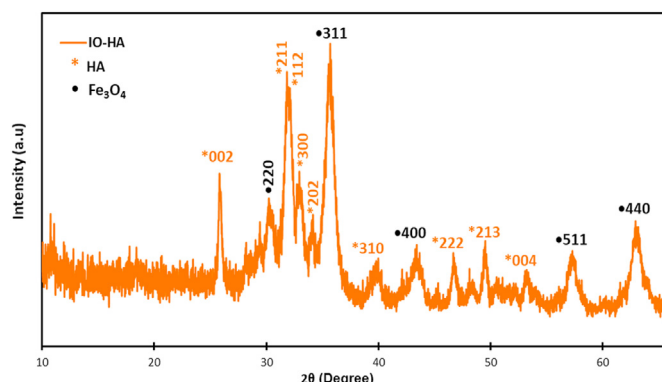


Figure 2. XRD pattern of IO-HA nanocomposite.

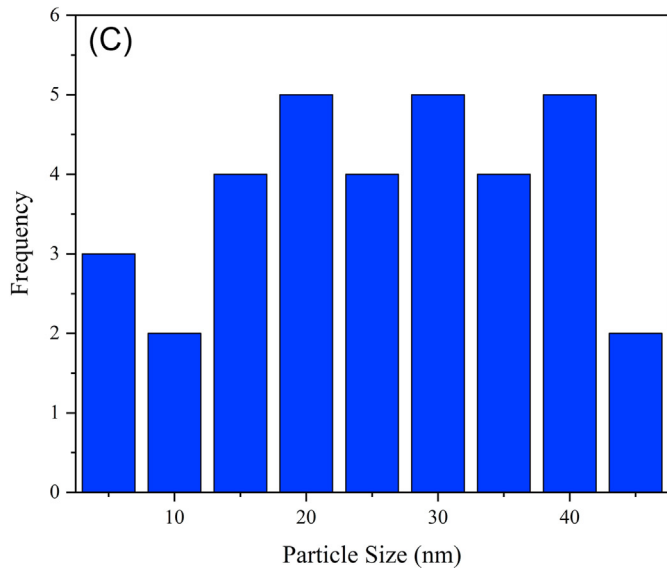
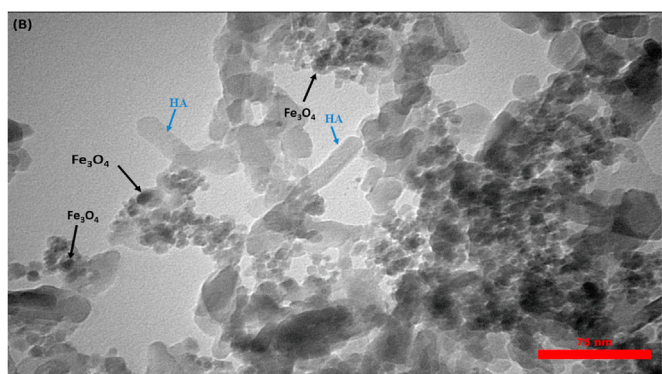
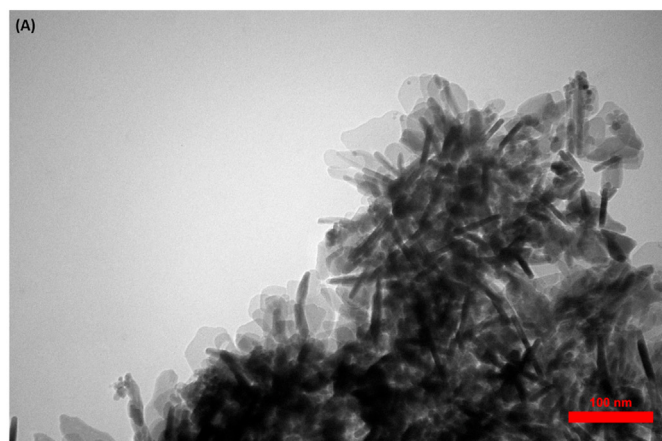


Figure 3. (A, B) TEM images of IO-HA nanocomposite and size distribution (C).

preserved in the final structure of the synthesized IO-HA nanocomposite without any impurity phases. The average crystal size was 10.5 nm.

TEM images of the synthesized nanocomposite showed in Figure 3 (A, B) that demonstrates the size of particles is in the range of 5–50 nm with rod-like in shape for HA. The rod-like morphology of the IO-HA, which is due to the hydroxyapatite part of the nanocomposite, as well as being iron oxide nanoparticles as black dots on the surfaces of the hydroxyapatite nanorods are quite clear [28,29]. The sample preparation for TEM observation may induce some aggregation of the magnetic particles

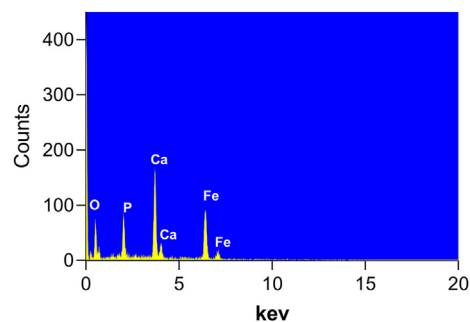


Figure 4. EDS spectrum of IO-HA nanocomposite.

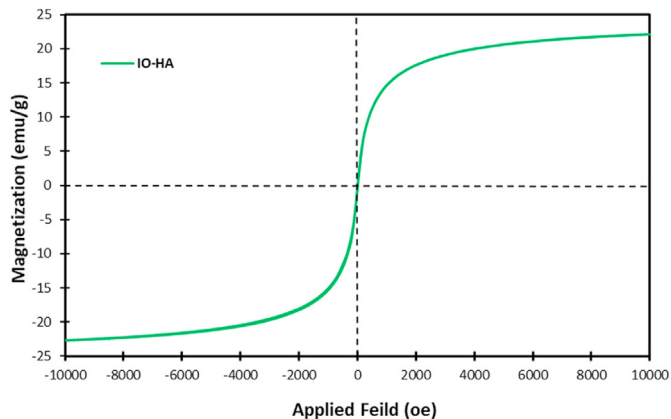


Figure 5. VSM graph of IO-HA nanocomposite.

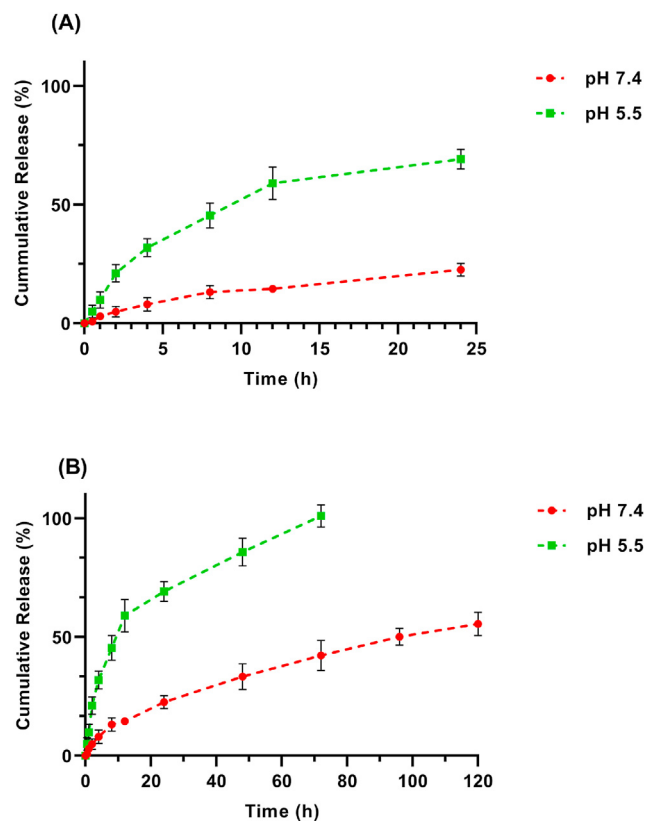


Figure 6. Cumulative release of loaded curcumin from IO-HA nanocomposite in different pH, (A) after 24 h, (B) after 120 h (n = 3).

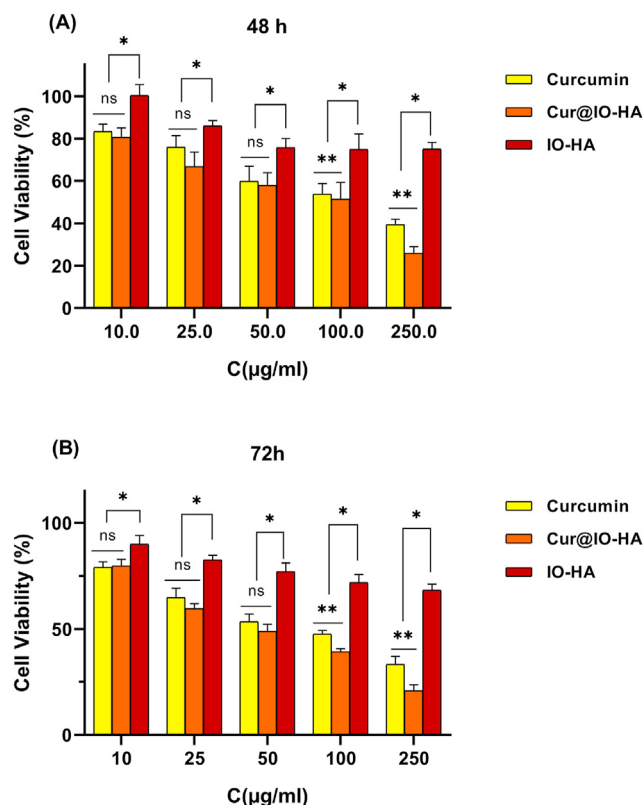


Figure 7. Cell viability assay of MCF-7 cells incubated with different concentrations of Curcumin, IO-HA, and Cur@IO-HA nanocomposite after (A) 48 h and (B) 72 h incubation.

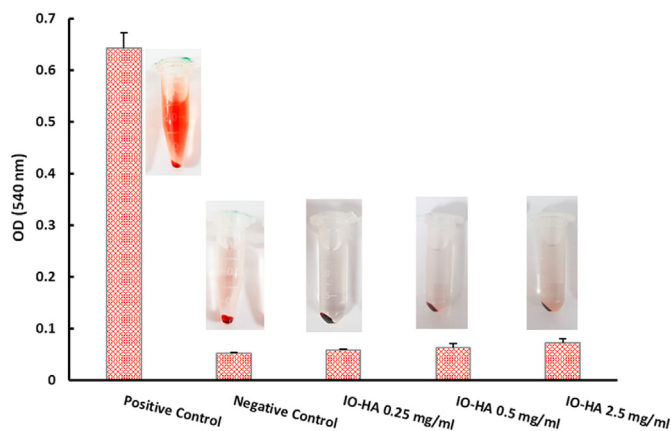


Figure 8. *In vitro* hemolysis assay of IO-HA nanocomposite with different concentrations, using deionized water as positive control and PBS (pH 7.4) as the negative control (n = 3).

during deposition on a grid, which is not unexpected due to the magnetic nature of the nanoparticles [30].

Further, the EDS analysis of IO-HA in Figure 4 provides the elemental composition of the synthesized nanocomposite consisting of iron (Fe), oxygen (O), calcium (Ca) and phosphorus (P). The data again confirm the presence of iron oxide and hydroxyapatite nanoparticles in the last IO-HA nanocomposite [2].

The magnetic behavior of IO-HA nanocomposite was investigated by the vibrating-sample magnetometer (VSM) with an applied magnetic field of -10 to +10 KOe. As can be seen in Figure 5, IO-HA nanocomposite has a saturation magnetization (M_s) of 22.2 emu/g with zero coercivity (H_c) which shown superparamagnetic behavior. The result indicates that

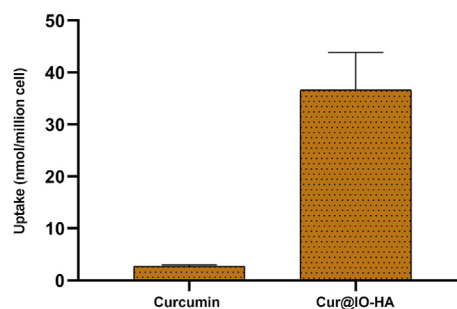


Figure 9. Cellular uptake of MCF-7 cells after 6 h incubation with free curcumin and Cur@IO-HA.

despite the hydroxyapatite coating of Fe_3O_4 nanoparticles, the magnetic properties of the synthesized nanocomposite is favorable [31]. The VSM result shows that nanoparticles have adequate magnetic properties to display a high enough magnetic response to direct the particles to a specific location in the body.

3.2. Release study

The release of curcumin from the synthesized nanocomposite was performed in phosphate buffer saline (PBS) with different pH values (pH 7.4 and 5.5) at 37 °C. The cumulative release (%) is given by the amount of curcumin released in PBS solution as a function of time. Figure 6 shows the controlled release profile of curcumin loaded IO-HA nanocomposite (Cur@IO-HA). At pH = 7.4, drug release is slower than in acidic conditions (Figure 6 A). The maximum release of curcumin occurred at pH 5.5 and after 72 h, the loaded drug was completely released, while in pH 7.4, after 72 h about 42% of load curcumin was released and after 120 h, the amount of cumulative release is about 55% (Figure 6 B). The reason for the further release of the loaded curcumin at pH 5.5 is the degradation of hydroxyapatite in this medium. In an acidic medium, hydroxyapatite decomposes to its constituent ions, calcium, and phosphate, enhances the release of the loaded drug at lower pH value. According to these data and by considering the decomposition of the synthesized nanocomposite structure to the acidic pH, it can be concluded that IO-HA has a potential efficiency to be a pH-sensitive drug carrier.

3.3. Cytotoxicity assay with MTT

To investigate the usability of the prepared nanocomposite in the field of medicine, the evaluation of toxicity and harmful effects on biological systems is essential. For this purpose, MTT assay was performed to evaluate the cytotoxicity of IO-HA and drug-carrier nanocomposite (Cur@IO-HA) comparing with the free curcumin on MCF7 breast cancer cell line in time intervals of 48 and 72 h with different concentrations. As can be seen from Figure 7, even after 72 h of incubation, IO-HA nanocomposite displayed about 70% cell viability even in the highest concentration so it can be concluded that the observed toxicity of curcumin loaded nanocomposite, Cur@IO-HA, caused by the released drug from the nanoparticles.

3.4. Blood compatibility of IO-HA nanocomposite

The blood compatibility of the synthesized nanocomposite is a clear criterion that could suggest it can be used in biomedical and pharmaceutical applications. The results of the hemolysis assay on IO-HA nanocomposite at concentrations of 0.25, 0.5, and 2.5 mg/ml compared to the positive and negative control sample are shown in Figure 8. There is no significant red blood cell lysis after 4 h of incubation with different concentrations of IO-HA at 37 °C, which can be concluded that the synthesized magnetic nanocomposite is fully compatible with red blood cells. By calculating the hemolysis percentage of red blood cells

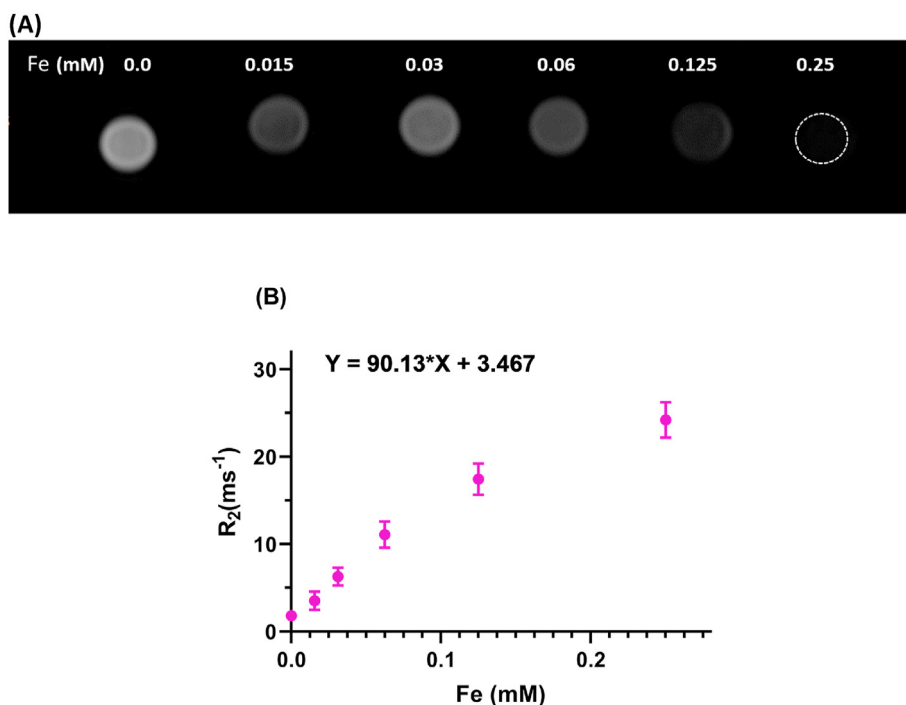


Figure 10. (A) T2-weighted MR phantom images of IO-HA nanocomposite. (B) The plot of R_2 against Fe concentration of IO-HA.

at different concentrations, it was found that the red blood cell lysis rate was less than 3.0%, even at the highest concentration of the nanocomposite, again emphasizing the lack of red blood cell lysis in the range of used concentrations.

3.5. Cellular uptake of IO-HA nanocomposite

For a nano-drug system to work, it must penetrate the target cell. It is also important to increase the uptake of drug nanoparticles by cancerous cells to treat the disease [3]. For this purpose, the cellular uptake of the synthesized nanocomposite was studied and curcumin has been used as a marker because of its fluorescence characteristic. As can be seen in Figure 9, the cellular uptake of MCF-7 cells after 6 h of exposure to free curcumin comparing Cur@IO-HA is very low. When MCF-7 cells exposed to Cur@IO-HA, the fluorescence intensity rose definitely (>10-fold) which confirms that the nano-drug had an acceptable cell entry compared to the free.

3.6. In vitro MRI studies

To investigate the MR properties of the synthesized nanocomposite, *in vitro* MRI measurements were carried out by a clinical 1.5 T MRI instrument with different concentrations ranging from 0.015 to 0.25 mM of Fe (determined by ICP-OES) prepared by dispersing IO-HA samples in agarose (1%). As shown in Figure 10 (A) increasing the concentration, the T2-weighted MR images became darker, which indicates that IO-HA nanocomposite potentially acts as an effective negative contrast agent. This result can be attributed to increasing the spin-spin relaxation time of water protons. The finding is confirmed by quantitative analysis of relaxation rate (R_2) over Fe concentration that is plotted in Figure 10 (B). The calculated relaxivity, r_2 , is 90.13 ± 7.7 , which is significantly high and implies that IO-HA nanocomposite can produce a T2 signal weakening effect.

4. Conclusion

In this study, a magnetic hydroxyapatite nanocomposite, IO-HA, was successfully prepared by the in-situ hydrothermal process prepared. The

TEM analysis confirms the IO-HA has a nanorod morphology. The sustained release of loaded curcumin from the synthesized nanocomposite reveals the excellent maximum release was obtained due to the degradation of the HA part of the nanocomposite in acidic media.

The more efficient cellular uptake of curcumin occurred when it was loaded to IO-HA nanocomposite. The results show that IO-HA has a suitable superparamagnetic property, making it favorable for magnetic resonance imaging purposes and the results of the *in vitro* MRI study confirmed it. Moreover, the synthesized nanocomposite caused no hemolytic and cytotoxic effects indicating its excellent biocompatibility. Therefore, IO-HA nanocomposite can be introduced as a theranostic T2-MRI contrast agent, which of course requires further studies in the *in vivo* condition.

Declarations

Author contribution statement

S. Sadighian: Conceived and designed the experiments.
M. Kermanian: Performed the experiments; Analyzed and interpreted the data; Wrote the paper.
M. Naghibi: Contributed reagents, materials, analysis tools or data.

Funding statement

This research did not receive any specific grant from funding agencies in the public, commercial, or not-for-profit sectors.

Competing interest statement

The authors declare no conflict of interest.

Additional information

No additional information is available for this paper.

Acknowledgements

This work was supported by the Zanjan University of Medical Sciences (Grant No. A-12-928-2).

References

- [1] S.C. McBain, H.H. Yiu, J. Dobson, Magnetic nanoparticles for gene and drug delivery, *Int. J. Nanomed.* 3 (2) (2008) 169.
- [2] S. Mondal, P. Manivasagan, S. Bharathiraja, M. Santha Moorthy, V. Nguyen, H. Kim, S. Nam, K. Lee, J. Oh, Hydroxyapatite coated iron oxide nanoparticles: a promising nanomaterial for magnetic hyperthermia cancer treatment, *Nanomaterials* 7 (12) (2017) 426.
- [3] Y. Huang, K. Mao, B. Zhang, Y. Zhao, Superparamagnetic iron oxide nanoparticles conjugated with folic acid for dual target-specific drug delivery and MRI in cancer theranostics, *Mater. Sci. Eng. C* 70 (2017) 763–771.
- [4] M.S. Laranjeira, A. Moco, J. Ferreira, S. Coimbra, E. Costa, A. Santos-Silva, P.J. Ferreira, F.J. Monteiro, Different hydroxyapatite magnetic nanoparticles for medical imaging: its effects on hemostatic, hemolytic activity and cellular cytotoxicity, *Colloids Surf. B Biointerfaces* 146 (2016) 363–374.
- [5] S. Pal, N.R. Jana, Pharmacologic vitamin C-based cell therapy via iron oxide nanoparticle-induced intracellular fenton reaction, *ACS App. Nano Mater.* (2020).
- [6] F. Ye, S. Laurent, A. Fornara, L. Astolfi, J. Qin, A. Roch, A. Martini, M.S. Toprak, R.N. Muller, M. Muhammed, Uniform mesoporous silica coated iron oxide nanoparticles as a highly efficient, nontoxic MRI T2 contrast agent with tunable proton relaxivities, *Contrast Media Mol. Imaging* 7 (5) (2012) 460–468.
- [7] P. Boehm-Sturm, A. Haackel, R. Hauptmann, S. Mueller, C.K. Kuhl, E.A. Schellenberger, Low-molecular-weight iron chelates may be an alternative to gadolinium-based contrast agents for T1-weighted contrast-enhanced MR imaging, *Radiology* 286 (2) (2018) 537–546.
- [8] Z.R. Stephen, F.M. Kievit, M. Zhang, Magnetite nanoparticles for medical MR imaging, *Mater. Today* 14 (7–8) (2011) 330–338.
- [9] J. Estelrich, M.J. Sánchez-Martín, M.A. Busquets, Nanoparticles in magnetic resonance imaging: from simple to dual contrast agents, *Int. J. Nanomed.* 10 (2015) 1727.
- [10] H. Shokrollahi, Structure, synthetic methods, magnetic properties and biomedical applications of ferrofluids, *Mater. Sci. Eng. C* 33 (5) (2013) 2476–2487.
- [11] G. Wang, S. Inturi, N.J. Serkova, S. Merkulov, K. McCrae, S.E. Russek, N.K. Banda, D. Simberg, High-relaxivity superparamagnetic iron oxide nanoworms with decreased immune recognition and long-circulating properties, *ACS Nano* 8 (12) (2014) 12437–12449.
- [12] Y. Luo, J. Yang, Y. Yan, J. Li, M. Shen, G. Zhang, S. Mignani, X. Shi, RGD-functionalized ultrasmall iron oxide nanoparticles for targeted T1-weighted MR imaging of gliomas, *Nanoscale* 7 (34) (2015) 14538–14546.
- [13] E.B. Ansar, M. Ajeesh, Y. Yokogawa, W. Wunderlich, H. Varma, Synthesis and characterization of iron oxide embedded hydroxyapatite bioceramics, *J. Am. Ceram. Soc.* 95 (9) (2012) 2695–2699.
- [14] N.A. Aval, J.P. Islamian, M. Hatamian, M. Arabfirouzjaei, J. Javadpour, M.-R. Rashidi, Doxorubicin loaded large-pore mesoporous hydroxyapatite coated superparamagnetic Fe₃O₄ nanoparticles for cancer treatment, *Int. J. Pharm.* 509 (1–2) (2016) 159–167.
- [15] P. Mi, D. Kokuryo, H. Cabral, M. Kumagai, T. Nomoto, I. Aoki, Y. Terada, A. Kishimura, N. Nishiyama, K. Kataoka, Hydrothermally synthesized PEGylated calcium phosphate nanoparticles incorporating Gd-DTPA for contrast enhanced MRI diagnosis of solid tumors, *J. Contr. Release* 174 (2014) 63–71.
- [16] Q. Fu, E. Saiz, M.N. Rahaman, A.P. Tomsia, Toward strong and tough glass and ceramic scaffolds for bone repair, *Adv. Funct. Mater.* 23 (44) (2013) 5461–5476.
- [17] Y.-J. Xu, L. Dong, Y. Lu, L.-C. Zhang, D. An, H.-L. Gao, D.-M. Yang, W. Hu, C. Sui, W.-P. Xu, Magnetic hydroxyapatite nanoworms for magnetic resonance diagnosis of acute hepatic injury, *Nanoscale* 8 (3) (2016) 1684–1690.
- [18] H. Xiong, S. Du, J. Ni, J. Zhou, J. Yao, Mitochondria and nuclei dual-targeted heterogeneous hydroxyapatite nanoparticles for enhancing therapeutic efficacy of doxorubicin, *Biomaterials* 94 (2016) 70–83.
- [19] W. Sun, J. Fan, S. Wang, Y. Kang, J. Du, X. Peng, Biodegradable drug-loaded hydroxyapatite nanotherapeutic agent for targeted drug release in tumors, *ACS Appl. Mater. Interfaces* 10 (9) (2018) 7832–7840.
- [20] G. Bharath, D. Prabhu, D. Mangalaraj, C. Viswanathan, N. Ponpandian, Facile in situ growth of Fe₃O₄ nanoparticles on hydroxyapatite nanorods for pH dependent adsorption and controlled release of proteins, *RSC Adv.* 4 (92) (2014) 50510–50520.
- [21] S. Mondal, P. Manivasagan, S. Bharathiraja, M.S. Moorthy, H.H. Kim, H. Seo, K.D. Lee, J. Oh, Magnetic hydroxyapatite: a promising multifunctional platform for nanomedicine application, *Int. J. Nanomed.* 12 (2017) 8389.
- [22] M.M. Yallapu, S.F. Othman, E.T. Curtis, N.A. Bauer, N. Chauhan, D. Kumar, M. Jaggi, S.C. Chauhan, Curcumin-loaded magnetic nanoparticles for breast cancer therapeutics and imaging applications, *Int. J. Nanomed.* 7 (2012) 1761.
- [23] A. Ramazani, M. Abrvash, S. Sadighian, K. Rostamizadeh, M. Fathi, Preparation and characterization of curcumin loaded gold/graphene oxide nanocomposite for potential breast cancer therapy, *Res. Chem. Intermed.* 44 (12) (2018) 7891–7904.
- [24] H. Rashidzadeh, M. Salimi, S. Sadighian, K. Rostamizadeh, A. Ramazani, In vivo antiproliferative activity of curcumin-loaded nanostructured lipid carriers, *Curr. Drug Deliv.* 16 (10) (2019) 923–930.
- [25] C. Gong, C. Wang, Y. Wang, Q. Wu, D. Zhang, F. Luo, Z. Qian, Efficient inhibition of colorectal peritoneal carcinomatosis by drug loaded micelles in thermosensitive hydrogel composites, *Nanoscale* 4 (10) (2012) 3095–3104.
- [26] S. Sadighian, K. Rostamizadeh, M.-J. Hosseini, M. Hamidi, H. Hosseini-Monfared, Magnetic nanogels as dual triggered anticancer drug delivery: toxicity evaluation on isolated rat liver mitochondria, *Toxicol. Lett.* 278 (2017) 18–29.
- [27] S. Sadighian, M. Abbasi, S. Arjmandi, H. Karami, Dye removal from water by zinc ferrite-graphene oxide nanocomposite, *Prog. Color Colorants Coat* 11 (2018) 85–92.
- [28] D.N. Thanh, P. Novák, J. Vejpravova, H.N. Vu, J. Lederer, T. Munshi, Removal of copper and nickel from water using nanocomposite of magnetic hydroxyapatite nanorods, *J. Magn. Magn. Mater.* 456 (2018) 451–460.
- [29] S. Venkateswarlu, B.N. Kumar, B. Prathima, Y. SubbaRao, N.V.V. Jyothi, A novel green synthesis of Fe₃O₄ magnetic nanorods using Punica Granatum rind extract and its application for removal of Pb (II) from aqueous environment, *Arabian J. Chem.* 12 (4) (2019) 588–596.
- [30] Ü. Dogan, H. Çiftçi, D. Cetin, Z. Suludere, U. Tamer, Nanoparticle embedded chitosan film for agglomeration free TEM images, *Microsc. Res. Tech.* 80 (2) (2017) 163–166.
- [31] C. Belviso, E. Agostinelli, S. Belviso, F. Cavalcante, S. Pascucci, D. Peddis, G. Varvaro, S. Fiore, Synthesis of magnetic zeolite at low temperature using a waste material mixture: fly ash and red mud, *Microporous Mesoporous Mater.* 202 (2015) 208–216.